Life-Cycle of Structures and Infrastructure Systems – Biondini & Frangopol (Eds)

Structural response of corroded concrete columns with different rebar confinements under cyclic compressive loading

H.O. Aminulai, N.S. Ferguson & M.M. Kashani
University of Southampton, Southampton UK

ABSTRACT: The new codes have recently introduced seismic detailing for new structures, but there are still older reinforced concrete structures without proper ductile detailing for earthquake resistance. These structures are further impacted by the corrosion of their embedded rebars which further reduces the strength and ductility under loading. This paper presents summary of the results of an experimental investigation performed on short RC columns, with different confinement configurations subject to varying degrees of corrosion, to investigate the structural responses to cyclic loading. The experiment was conducted on 20 short RC columns (square and circular) with two levels of confinements and steel reinforcement corrosion loss ranging from 0% to to ~30% subjected to cyclic compressive load. The test results show that corrosion and rebar confinements significantly impact the structural responses of corroded columns.

1 INTRODUCTION

Reinforced concrete (RC) columns are commonly used to construct civil engineering structures. They are affected by factors such as dry and wet cycles, freeze-thaw cycles, ageing of the materials, and the corrosion of reinforcement steel (Chen et al., 2022, Luo et al., 2020). Among all these factors, steel corrosion has been the most devastating, with chloride-induced corrosion the most severe, leading to catastrophic failure and collapse of structures (Ma et al., 2022). The corrosion of reinforcements in RC members significantly degrades their structural performance leading to structures with reduced load-carrying capacity, ductility and structural safety (Biswas et al., 2020). Furthermore, corrosion significantly reduces the confinement effectiveness of transverse bars and the buckling resistance of longitudinal bars in RC columns, especially structures in severely corrosive environments and subjected to seismic loading (Luo et al., 2020).

Numerous old RC and steel bridges in the marine environment and cold regions (using deicing salt) are suffering from steel corrosion resulting in the durability degradation of RC bridges (Akiyama et al., 2011, Ou et al., 2013, Kashani et al., 2019, Ni Choine et al., 2016). In addition, these bridges are designed with the old codes without proper confinement detailing and seismic resistance, making them vulnerable to collapse under seismic excitation.

While several studies have been dedicated to investigating the structural vulnerability of corrosion-damaged RC members, there is paucity in the literature on the influence of corrosion damage, confinement levels and cross-sectional shape on the seismic behaviour of ageing RC bridge columns/piers. Several numerical and analytical models have been used to investigate the effect of corrosion and transverse reinforcement confinements on RC members' seismic response and failure (Kashani et al., 2016a, Kashani et al., 2016b, Kashani et al., 2018, Su et al., 2015). However, these works have mostly not been validated with experimental tests. Therefore, there is a need for experimental investigation of the seismic response of corroded RC columns to corrosion damage and inadequate confinements under cyclic compressive loading.

Cyclic experiments are a major method to provide insight into the seismic performance of the structural component. However, although it is recognised that the corrosion-induced

DOI: 10.1201/9781003323020-408

damage on coastal bridge piers significantly affects the safety of the structures during the long-term service period, the damage mechanism and the mechanical behaviour are still seldom understood. This paper investigates the effect of corrosion and confinement on the cyclic performance of ageing low-strength concrete RC columns.

2 EXPERIMENTAL CAMPAIGN

2.1 *Specimen preparation and material characterisation*

Twenty RC columns (ten squares and ten circulars) with five targeted corrosion mass losses (0%, 5%, 10%, 20% and 30%) and two confinement ratios, high (L/D=5) and low (L/D=13), were used and labelled as shown in Table 1. All the columns have the same length (600mm), with the square columns having 125 × 125mm cross-section incorporating 4 Φ10mm longitudinal bars, while the circular columns are 125mm diameter with 5 Φ10mm longitudinal bars. The columns are confined with Φ6mm stirrups in the middle 400mm zone, while the 100mm ends have the stirrups at 25mm spacings. Furthermore, the 100mm ends were strengthened with epoxy-coated GFRP to prevent localised damage at the top and bottom ends of the columns and ensure that the failure occurs at the 400mm middle zone.

Table 1. Experimental test matrix.

Circular columns			Square columns		
Specimen label	Confinement level	Targeted corrosion (%)	Specimen label	Confinement level	Targeted corrosion (%)
C5A0	5	0	S5A0	5	0
C5A5	5	5	S5A5	5	5
C5A10	5	10	S5A10	5	10
C5A20	5	20	S5A20	5	20
C5A30	5	30	S5A30	5	30
C13A0	13	0	S13A0	13	0
C13A5	13	5	S13A5	13	5
C13A10	13	10	S13A10	13	10
C13A20	13	20	S13A20	13	20
C13A30	13	30	S13A30	13	30

The concrete was designed as low-strength concrete representing ageing columns with an expected mean compressive strength of 20MPa. Concrete samples with the same configuration as the square and circular columns were collected during the casting to determine the actual strength of the concrete. The test was done with the servo-hydraulic 630kN Instron Schenk machine at the Testing and Structures Research Laboratory (TSRL), University of Southampton. The average compressive strengths of the concrete are 13.8MPa and 12.6Mpa for the square and circular columns, respectively.

2.2 *Accelerated corrosion procedure*

The electrochemical method was applied to the corrosion process to hasten corrosion process in the laboratory. This method has been shown to have similar results as natural corrosion (Hou et al., 2019, Mak et al., 2019, Yuan et al., 2007).

The rebars were joined together and connected to the anode, while the stainless steel sheet was linked with the cathode of the direct current (DC) power supply. The power supply was adjusted to supply a constant current of 2Amp for the corrosion of the rebars in the columns submerged in 10% sodium chloride solution (Figure 1(a-b)). Faraday's 2nd law of electrolysis (Equation 1) was used to estimate the expected corrosion mass loss by calculating the duration to achieve such mass loss (Kashani et al., 2013a). The actual mass loss, γ, is estimated at the

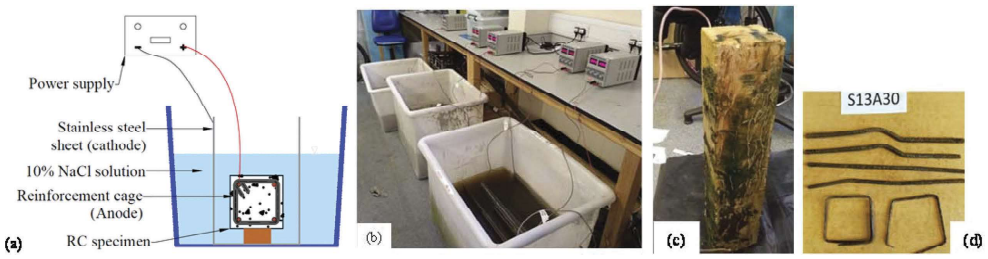

Figure 1. Accelerated corrosion procedure; (a) Schematic setup drawing, (b) laboratory setup (c) corroded columns after completion of corrosion and (d) corroded rebars after cleaning.

end of testing by weighing the rebars after removing and cleaning the rust (Figure 1(c-d)) and concrete from the surface (Equation 2). Equation 2 gives an average corrosion loss (mass loss) along the length of the rebar.

$$m_l = \frac{MIT}{ZF} \tag{1}$$

$$\gamma = \frac{m_0 - m}{m_0} \times 100 \tag{2}$$

where m_l = estimated mass loss (g), M = molar mass of the iron (56g/mol), Z = ionic charge for iron (Z=2), F = Faraday's constant (96500 C/mol), I = applied current (Ampere, A), T = estimated time to achieve the desired corrosion (s), m_0, = mass per unit length of the uncorroded rebar, and m = mass per unit length after cleaning.

2.3 *Cyclic loading protocol and instrumentation*

The RC columns were tested under axial compressive cyclic loading. The loading protocol was set to have 20 cycles with ten different mean strains, each strain peak repeating twice, as shown in Figure 2. The mean strain was estimated from the displacement values of a similar experimental test done on corroded RC under monotonic loading. The first five lower strain peaks were applied at 0.1mm/sec loading rate while the remaining peaks were at 0.15mm/sec. The cyclic loading protocol was set up using the Instron Wavematrics software.

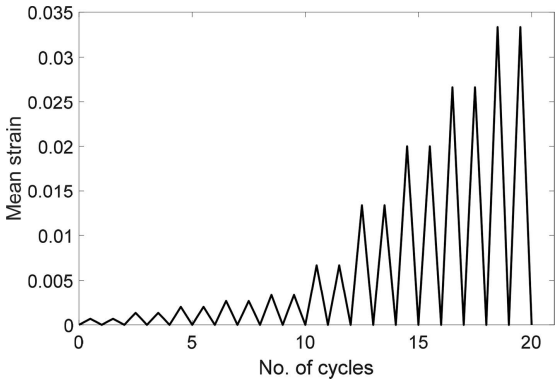

Figure 2. Cyclic compressive loading protocol.

3 EXPERIMENTAL SETUP

The RC columns were tested under axial cyclic compressive load using displacement control with a lower loading rate for the first ten cycles. After that, the remaining cycles were at a slightly higher rate. Also, the test is conducted under complete axial cyclic compression loading, with each loading cycle repeated twice without going into the tension zone. The setup of the experiment is shown in Figure 3(a). The displacement at the middle 400mm zone of the RC columns is

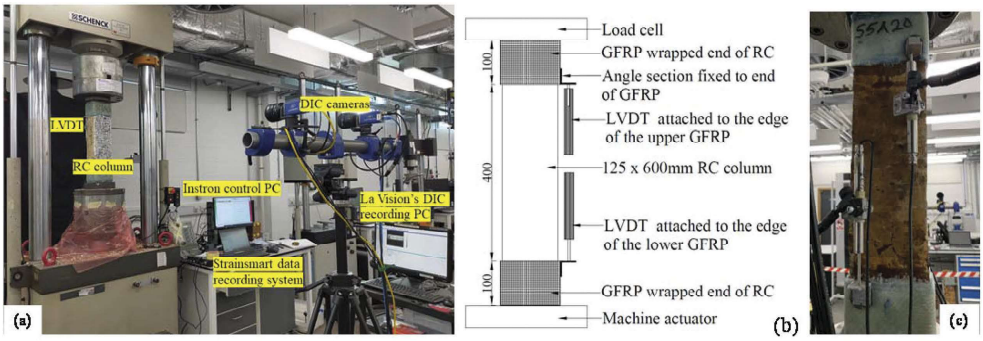

Figure 3. Experimental test setup (a) laboratory setup; (b) schematic of the LVDT connection; (c) Image of the LVDT connections to the RC samples.

measured with the Linear Variable Differential Transformers (LVDTs) fixed to the edge of the Glass fibre-reinforced polymers (GFRP) strengthened ends (Figures 3(b) and 3(c)). This ensures that the LVDTs measure the axial deformations in the differently confined 400mm section of the columns, which are recorded via a data acquisition unit (Strainsmart 8000).

4 EXPERIMENTAL RESULTS

4.1 *Calculation of corrosion and mass loss ratio*

The actual mass losses resulting from the accelerated corrosion process estimated from Equation 2 are presented in Figure 4. The results showed that the transverse bars had more severe corrosion than the longitudinal bars under the same constant current and duration (Li et al., 2022) in all the columns.

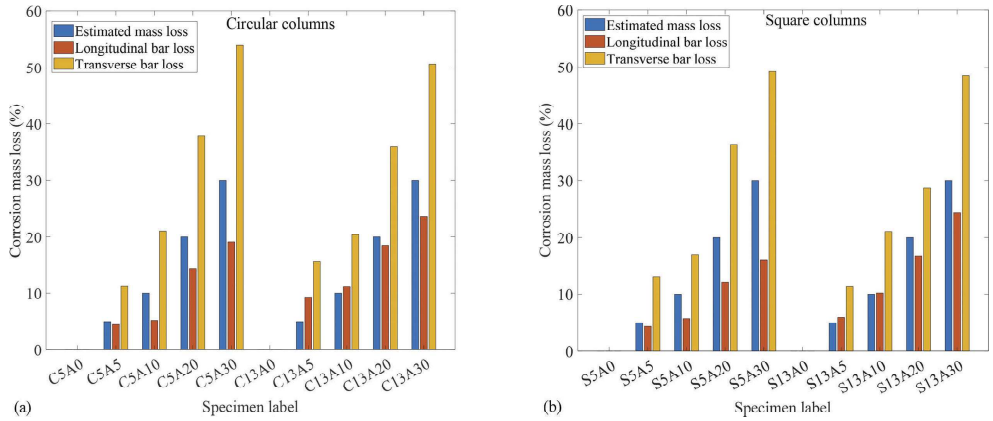

Figure 4. Accelerated corrosion mass loss for the RC columns (a) circular and (b) square.

This mass loss results from the closeness of the transverse bars to the surface of the concrete, leading to a higher concentration of chloride ions and an early start of corrosion (Gu et al., 2020). Furthermore, the diameter of the longitudinal rebar (10mm) was greater than that of the stirrups (6mm). In this regard, the mass loss ratio of transverse stirrups with smaller diameters was higher than that of the longitudinal rebar, according to Faraday's second law of electrolysis (Kashani, 2017).

4.2 *Axial cyclic testing of the RC columns*

The stress-strain responses of the RC columns to the applied axial cyclic compressive load are presented in Figure 5(a-h). The observed cyclic responses of the RC columns are similar at the elastic range until yield and afterwards becomes nonlinear beyond the peak stress due to the corrosion and confinements of the rebars. The hysteretic curve of the corroded columns within each

confinement's configuration was compared with the non-corroded ones. It showed a gradual decrease in the strength, stiffness and ductility of the columns as the corrosion increased. Consequently, columns with very close mass loss have their maximum strengths relative to each other, especially at low corrosion between 5% and 10% (Figure 5(a, c, e and g)). For example, the strength loss between the highly confined circular columns (Figure 5(a-b)) was reduced by 13%, 22%, 26%, and 37% for the 5%, 10%, 20% and 30% estimated mass loss, respectively. This trend is also observed in the lowly confined (L/D=13) columns having between 10% to 48% reduction (Figure 5(c-d)).

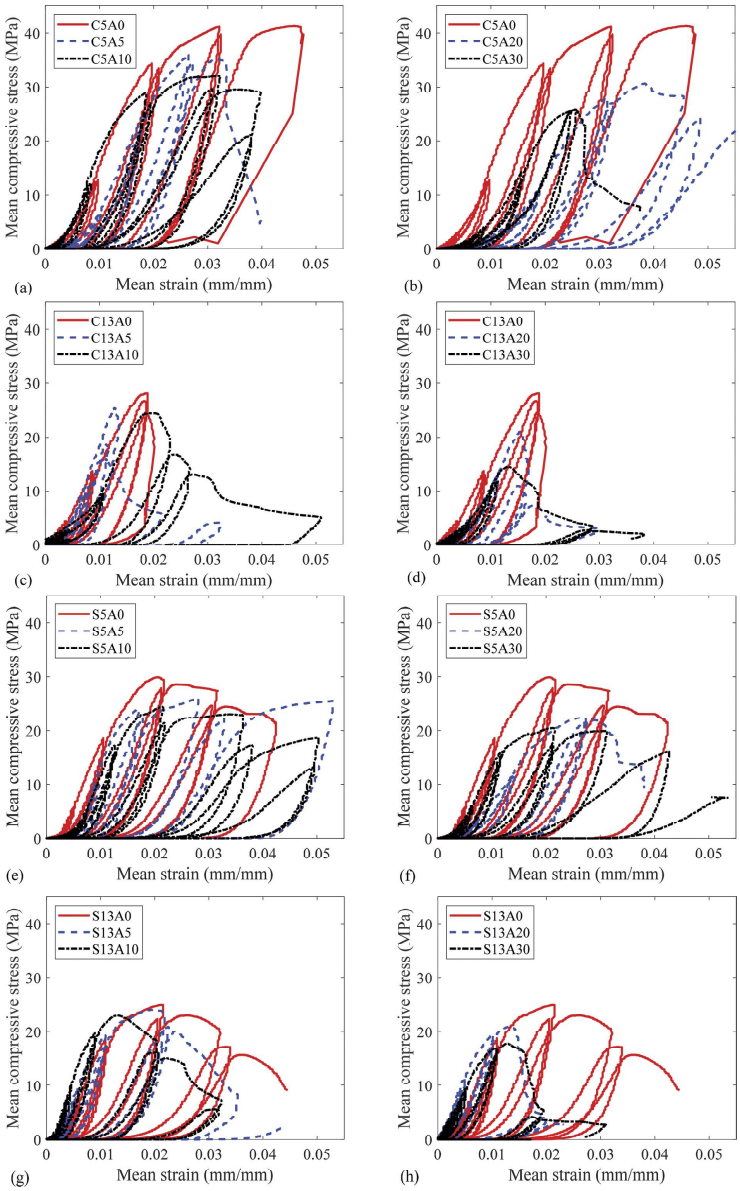

Figure 5. Axial cyclic stress-strain response of the RC columns; circular (L/D = 5 (a-b) and L/D = 13 (c-d)) and square (L/D = 5 (e-f) and L/D = 13 (g-h)).

4.3 *Impact of corrosion on energy dissipation capacity*

The plots of the normalised accumulated hysteretic energy dissipated by the RC columns against the number of cycles are presented in Figure 6(a-d). The graphs showed similar behaviour for all the columns, with very low energy dissipated at the smaller loading cycles (low strain loading rates) and a steep increase in the energy dissipated after the 10th cycle. The steep increase in the dissipated energy is more significant at high corrosion and low confinement in both the circular and square columns.

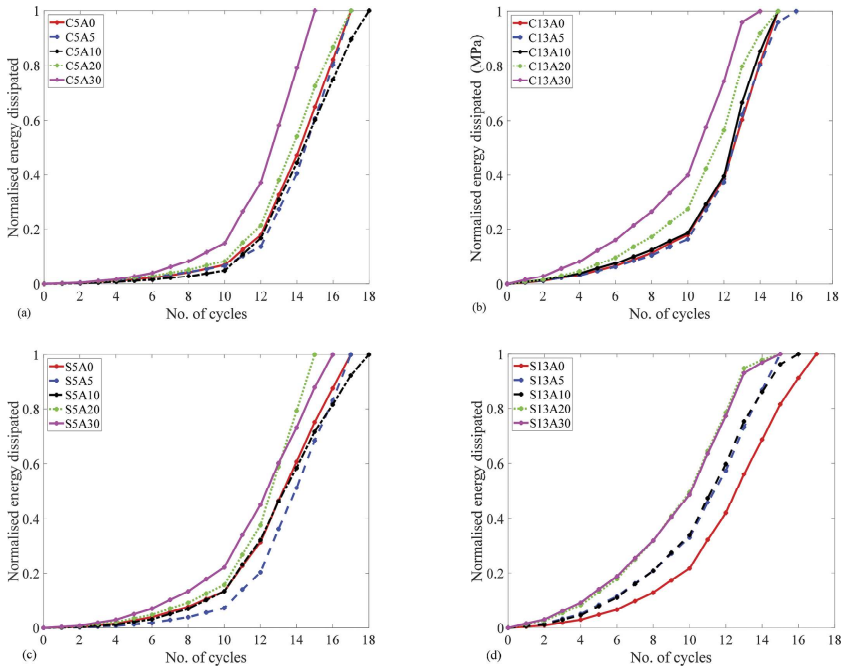

Figure 6. Normalised dissipated energy of the RC columns; circular ((a) L/D = 5, (b) L/D = 13)); square ((c) L/D = 5, and (d) L/D = 13)).

4.4 *Impact of corrosion on buckling of vertical reinforcement*

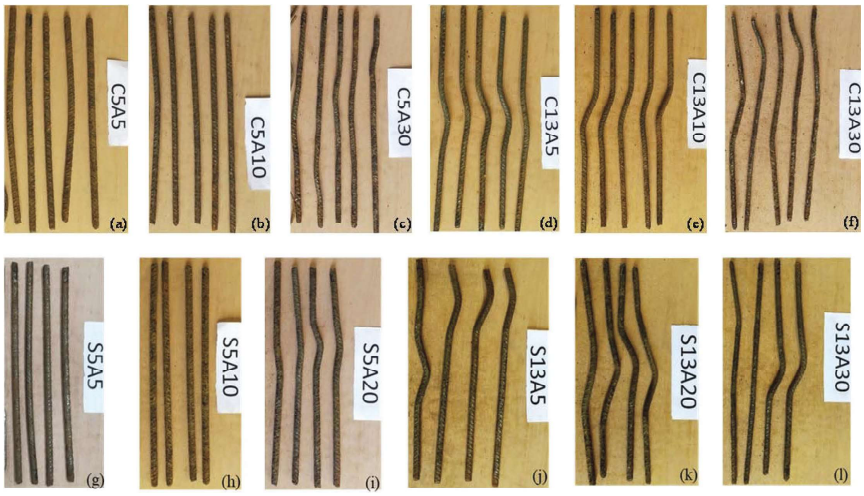

Figure 7. Observed buckling failure of the longitudinal reinforcement in the RC columns. Circular; L/D = 5 (a-c), and L/D = 13 (d-f), square; L/D = 5 (g-i), and L/D = 13 (d-f).

The corrosion and confinement of rebars affect the buckling behaviour of the longitudinal bars. This buckling is more pronounced in bars with pitting corrosion, resulting in a localised reduction of the cross-section area along the corroded bar (Kashani et al., 2013a). As a result, the bars in the highly confined circular columns had less buckling at low corrosion (Figure 7(a-b)). Conversely, the buckling of the rebars in the highly confined columns is more pronounced at high corrosion (Figure 7(d)), where the effect of pitting corrosion is prevalent (Kashani et al., 2013b, Kashani, 2017). Furthermore, the buckling of the rebars in the lowly confined columns is more severe even at low corrosion levels from the combination of corrosion and inadequate confinement of the column (Figure 7(d-f)). Similar behaviour is observed in the buckling response of the square columns (high confined Figure 7(g-i) and low confined (Figure 7(j-l)).

5 CONCLUSIONS

Twenty RC column specimens with five different reinforcement corrosion levels and two confinement configurations were tested under axial cyclic compressive load. Moreover, the relationship between the seismic behaviour, such as rebar corrosion loss ratio, ultimate strength, normalised dissipated energy, and inelastic buckling of rebar, was investigated. The following conclusions can be drawn from this study.

Transverse reinforcement showed much higher vulnerability to chloride-induced deterioration in the RC columns than the respective longitudinal reinforcement. Consequently, the ultimate failure of the columns reduced as corrosion damage increased and confinement effectiveness was diminished. Well-confined specimens showed a lesser loss in strength and deformability after corrosion than under-confined specimens.

Corrosion of transverse confining steel affects the strength and deformability of confined concrete. The effectiveness of confinement reinforcements in confining the core concrete reduces as the corrosion increases. Higher corrosion levels and low confinement lead to more severe degradation of the seismic behaviour of RC columns. The highly corroded columns, where the corrosion loss ratio is 20–30%, have reduced seismic response: poor hysteretic response, stiffness degradation, steep descending branch in the envelope curve, and energy dissipation reduction. It can be concluded that the design of new confined concrete elements should consider the possible/anticipated loss due to corrosion during the structure's life to enable a safe ductile response, which is crucial in earthquake-prone regions.

REFERENCES

Akiyama, M., Frangopol, D. M. & Matsuzaki, H. 2011. Life-cycle reliability of RC bridge piers under seismic and airborne chloride hazards. *Earthquake Engineering & Structural Dynamics*, 40, 1671–1687.

Biswas, R. K., Iwanami, M., Chijiwa, N. & Uno, K. 2020. Effect of non-uniform rebar corrosion on structural performance of RC structures: A numerical and experimental investigation. *Construction and Building Materials*, 230, 116908.

Chen, J., Wang, Z., Xu, A. & Zhou, J. 2022. Compressive Behavior of Corroded RC Columns Strengthened With Ultra-High Performance Jacket. *Frontiers in Materials*, 9, 1–14.

Gu, X.-L., Dong, Z., Yuan, Q. & Zhang, W.-P. 2020. Corrosion of Stirrups under Different Relative Humidity Conditions in Concrete Exposed to Chloride Environment. *Journal of Materials in Civil Engineering*, 32, 04019329.

Hou, L., Zhou, B., Guo, S., Aslani, F. & Chen, D. 2019. Corrosion behavior and flexural performance of reinforced concrete/ultrahigh toughness cementitious composite (RC/UHTCC) beams under sustained loading and shrinkage cracking. *Construction and Building Materials*, 198, 278–287.

Kashani, M. M. 2017. Size Effect on Inelastic Buckling Behavior of Accelerated Pitted Corroded Bars in Porous Media. *Journal of Materials in Civil Engineering*, 29, 04017022.

Kashani, M. M., Crewe, A. J. & Alexander, N. A. 2013a. Nonlinear cyclic response of corrosion-damaged reinforcing bars with the effect of buckling. *Construction and Building Materials*, 41, 388–400.

Kashani, M. M., Crewe, A. J. & Alexander, N. A. 2013b. Nonlinear stress–strain behaviour of corrosion-damaged reinforcing bars including inelastic buckling. *Engineering Structures*, 48, 417–429.

Kashani, M. M., Lowes, L. N., Crewe, A. J. & Alexander, N. A. 2016a. Computational Modelling Strategies for Nonlinear Response Prediction of Corroded Circular RC Bridge Piers. *Advances in Materials Science and Engineering*, 2016, 2738265.

Kashani, M. M., Lowes, L. N., Crewe, A. J. & Alexander, N. A. 2016b. Nonlinear fibre element modelling of RC bridge piers considering inelastic buckling of reinforcement. *Engineering Structures*, 116, 163–177.

Kashani, M. M., Maddocks, J. & Dizaj, E. A. 2019. Residual Capacity of Corroded Reinforced Concrete Bridge Components: State-of-the-Art Review. *Journal of Bridge Engineering*, 24, 1–16.

Kashani, M. M., Salami, M. R., Goda, K. & Alexander, N. A. 2018. Non-linear flexural behaviour of RC columns including bar buckling and fatigue degradation. *Magazine of Concrete Research*, 70, 231–247.

Li, Q., Dong, Z., He, Q., Fu, C. & Jin, X. 2022. Effects of Reinforcement Corrosion and Sustained Load on Mechanical Behavior of Reinforced Concrete Columns. *Materials (Basel)*, 15.

Luo, X., Cheng, J., Xiang, P. & Long, H. 2020. Seismic behavior of corroded reinforced concrete column joints under low-cyclic repeated loading. *Archives of Civil and Mechanical Engineering*, 20, 40.
Ma, J., Yu, L., Li, B. & Yu, B. 2022. Stress–strain model for confined concrete in rectangular columns with corroded transverse reinforcement. *Engineering Structures*, 267, 1–14.
Mak, M. W. T., Desnerck, P. & Lees, J. M. 2019. Corrosion-induced cracking and bond strength in reinforced concrete. *Construction and Building Materials*, 208, 228–241.
Ni Choine, M., Kashani, M. M., Lowes, L. N., O'connor, A., Crewe, A. J., Alexander, N. A. & Padgett, J. E. 2016. Nonlinear dynamic analysis and seismic fragility assessment of a corrosion damaged integral bridge. *International Journal of Structural Integrity*, 7.
Ou, Y.-C., Fan, H.-D. & Nguyen, N. D. 2013. Long-term seismic performance of reinforced concrete bridges under steel reinforcement corrosion due to chloride attack. *Earthquake Engineering & Structural Dynamics*, 42, 2113–2127.
Su, J., Wang, J., Bai, Z., Wang, W. & Zhao, D. 2015. Influence of reinforcement buckling on the seismic performance of reinforced concrete columns. *Engineering Structures*, 103, 174–188.
Yuan, Y., Ji, Y. & Shah, S. P. 2007. Comparison of two accelerated corrosion techniques for concrete structures. *ACI Structural Journal*, 104, 344–347.